PERGAMON

International Journal of Solids and Structures 36 (1999) 3917–3943

INTERNATIONAL JOURNAL OF SOLIDS and STRUCTURES

Design and fabrication of submerged cylindrical laminates—I

George J. Dvorak[a,*], Petr Prochazka[b], Mullahalli V. Srinivas[a]

[a] *Center for Composite Materials and Structures, Rensselaer Polytechnic Institute, Troy, NY 12180-3590, U.S.A.*
[b] *Department of Structural Mechanics, Faculty of Civil Engineering, Czech Technical University, Prague, Czech Republic*

Received 21 August 1997; in revised form 5 June 1998

Abstract

This is the first of a two-part paper concerned with both structural and fabrication process design of a closed-end laminated composite cylinder intended for service in deep sea environment. The cylinder is made of many different orthotropic layers and is loaded by uniform, axisymmetric surface tractions. In addition, piecewise uniform eigenstrains and residual stresses may be caused in the layers during fabrication, by fiber prestress for waviness reduction and by piecewise uniform changes in temperature. The overall goal is to assure efficient use of the composite structure under a prescribed hydrostatic pressure, and to select fiber prestress distribution such that the total stresses in the plies do not exceed certain strength magnitudes.

Mechanical and residual stresses in the layers are evaluated with mechanical and transformation influence functions. For the proportional loading applied by a hydrostatic pressure, a procedure is outlined for design of several layups such that the cylinder wall experiences an isotropic in-plane strain and, therefore, all layers support the same compressive normal stresses, regardless of fiber orientation. The results are applied in design and analysis stress fields in a specific structure. Fabrication process design is discussed in the second part of the paper (Srinivas et al., 1999, Int. J. Solids Structures, 36, 3945–3976). © 1999 Elsevier Science Ltd. All rights reserved.

1. Introduction

One of the potential applications of composite materials is in structures subjected primarily to compressive loads, such as submersibles. The incentive is the relatively high axial compressive strength that has been found in carefully fabricated thick samples, e.g., 1440 MPa (209 ksi) in AS4/3501-6 carbon/epoxy system (Daniel and Isahi, 1994); even the more frequently reported magnitude of about 700 MPa for this system is attractive. Cylindrical or spherical shapes are typically preferred in such applications, and if the wall thickness to diameter ratios are small, then, regardless of actual size, the structure responds to external hydrostatic compression as a thin-walled cylinder or sphere, with nearly uniform distribution of load-induced strains through the

* Corresponding author. Fax: 001 518 276 8784; e-mail: dvorak@rpi-edu

PII: S0020-7683(98)00181-4

wall thickness. However, significant residual stress gradients can be caused by fabrication and processing, for example, by fiber prestress to reduce fiber waviness. In superposition with external loads, such residual stresses may promote premature failure (Dvorak and Prochazka, 1996).

Of major concern in design of submerged structures is, of course, support of the external pressure which causes proportionally changing internal stress magnitudes at different depths. Under such loading, ply layup may be modified to adjust stiffness distribution in the structure such that all plies support the same axial compressive stress. Moreover, internal eigenstrains may be introduced into the plies to cause a desirable redistribution of internal stresses; either during fabrication or by suitable actuator devices in service.

This is the first of a two-part study of mechanical and residual stress and strain fields in multi-layer composite cylinders loaded by external pressure and by piecewise uniform eigenstrain distributions introduced in the layers during fabrication. Any number of different, cylindrically orthotropic elastic layers can be considered. The goal is to establish a theoretical framework for evaluation of the relevant fields in the individual layers of the structure, to describe minimum weight laminate layup designs for a specific material system, and to illustrate by examples the distributions of mechanical, thermal and residual fields. The second part of the study (Srinivas et al., 1999) presents analysis of fabrication procedures involving selected distributions of fiber prestress, and also describes procedures for determining prestress magnitudes in individual plies that create prescribed residual stress fields in the cylinder wall. Buckling analysis is not considered here, it can be found together with many related references in Kardomateas and Philobos (1995) and Kardomateas (1997).

In Sections 2–4, we derive local fields and overall response of the layered cylindrical structure under the external pressure and local eigenstrains. Section 5 presents derivation of the transformation influence functions (Dvorak and Benveniste, 1992; Dvorak, 1992) while Section 6 describes certain laminate layups for minimum weight design with a specific material system. Applications are summarized in Section 7.

2. The layered composite cylinder

A long cylindrical structure of circular cross-section consists of N concentric cylindrical layers, all located in the volume Ω with surface S. A cylindrical $r\theta z$ system of coordinates is defined according to Fig. 1, a Cartesian system X_i, $i = 1, 2, 3$, is also introduced for future use. The inner and outer boundaries of the structure are denoted as S_a at $r = a$, and S_b at $r = b$, respectively, $a < b$; and the end faces as S_z at $z = 0, L$. Similarly, for each layer (j), the inner and outer radii are denoted as $r = a_j$ and $r = b_j$; $a_j < b_j$. It follows that $b_j = a_{j+1}$ for $j = 1, 2, \ldots, N-1$, and that $a_1 = a$, $b_n = b$.

In an actual structure, each layer (j) represents a unidirectional fibrous ply where the fibers contain some constant angle ψ_j with the coordinate direction z. However, homogenized sublaminates consisting of many fibrous plies of a certain layup and stacking sequence may also be regarded as layers in the elastic analysis of mechanical load effects. To allow for these and other possible choices, the elastic symmetry of the layer is assumed to correspond to cylindrical orthotropy.

Attention will be limited to axisymmetric loading of the cylinder, such as external and internal

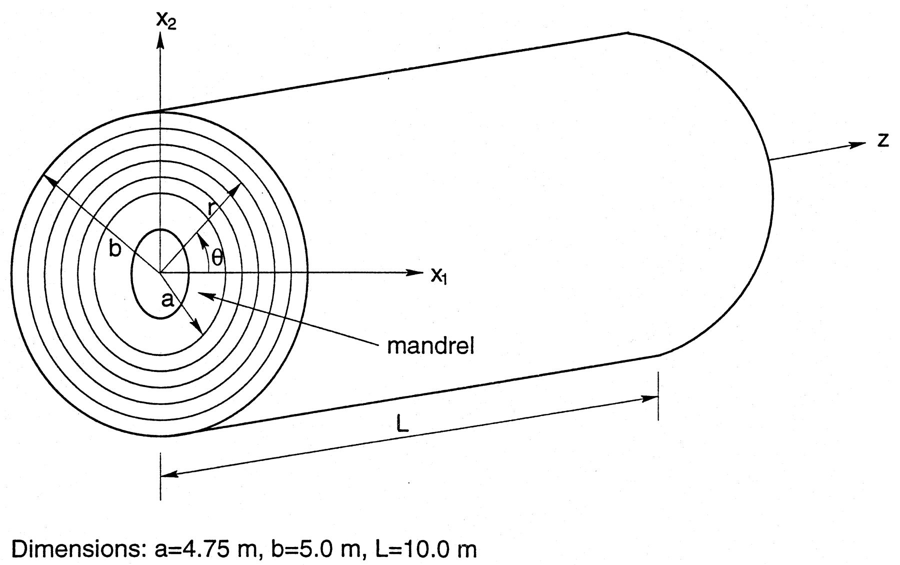

Fig. 1. Geometry of the layered composite cylinder.

radial pressure, and axial normal pressure. Moreover, we admit axisymmetric eigenstrains in the layers; these may be caused by many different processes, for example, by thermal changes, moisture absorption, inelastic deformation of the matrix during curing or under load, and by prestressing of the fibers in fabrication. Regardless of their origin, the eigenstrains are assumed to be uniform in the volume of each layer. Since the structure is also axisymmetric, it is sufficient to write the elastic constitutive relations for the material in each layer (j) only for the following strain, stress, and eigenstrain components,

$$\varepsilon^j = \begin{Bmatrix} \varepsilon^j_{rr} \\ \varepsilon^j_{\theta\theta} \\ \varepsilon^j_{zz} \end{Bmatrix} = \boldsymbol{M}^j \begin{Bmatrix} \sigma^j_{rr} \\ \sigma^j_{\theta\theta} \\ \sigma^j_{zz} \end{Bmatrix} + \begin{Bmatrix} \mu^j_{rr} \\ \mu^j_{\theta\theta} \\ \mu^j_{zz} \end{Bmatrix} = \boldsymbol{M}^j \boldsymbol{\sigma}^j + \boldsymbol{\mu}^j, \tag{1}$$

Here, the vector $\boldsymbol{\mu}^j$ denotes the uniform eigenstrains in the layer, and the compliance matrix of the cylindrically orthotropic material is written in terms of the elastic constants, defined in the $r\theta z$ coordinates, as

$$\boldsymbol{M}^j = \begin{bmatrix} M^j_{rr} & M^j_{r\theta} & M^j_{rz} \\ M^j_{\theta r} & M^j_{\theta\theta} & M^j_{\theta z} \\ M^j_{zr} & M^j_{z\theta} & M^j_{zz} \end{bmatrix} = \begin{bmatrix} \dfrac{1}{E^j_r} & -\dfrac{v^j_{r\theta}}{E^j_\theta} & -\dfrac{v^j_{rz}}{E^j_z} \\ -\dfrac{v^j_{\theta r}}{E^j_r} & \dfrac{1}{E^j_\theta} & -\dfrac{v^j_{\theta z}}{E^j_z} \\ -\dfrac{v^j_{zr}}{E^j_r} & -\dfrac{v^j_{z\theta}}{E^j_\theta} & \dfrac{1}{E_z} \end{bmatrix} \tag{2}$$

where $v^j_{r\theta}E^j_r = v^j_{\theta r}E^j_\theta$, etc., so that $M^j_{pq} = M^j_{qp}$; $p, q = r, \theta, z$.

The reciprocal of (1) is

$$\boldsymbol{\sigma}^j = \begin{Bmatrix} \sigma_{rr}^j \\ \sigma_{\theta\theta}^j \\ \sigma_{zz}^j \end{Bmatrix} = \boldsymbol{L}^j \begin{Bmatrix} \varepsilon_{rr}^j - \mu_{rr}^j \\ \varepsilon_{\theta\theta}^j - \mu_{\theta\theta}^j \\ \varepsilon_{zz}^j - \mu_{zz}^j \end{Bmatrix} = \boldsymbol{L}^j(\boldsymbol{\varepsilon}^j - \boldsymbol{\mu}^j) \tag{3}$$

with $\boldsymbol{L}^j$ satisfying $\boldsymbol{L}^j\boldsymbol{M}^j = \boldsymbol{I}$, a (3×3) identity matrix. In terms of Young's moduli and Poisson's ratios of the layer material, the coefficients of $\boldsymbol{L}^j$ evaluate as

$$L_{rr}^j = \frac{E_r(1-v_{\theta z}v_{z\theta})}{D_\mathrm{o}} \quad L_{\theta\theta}^j = \frac{E_\theta(1-v_{rz}v_{zr})}{D_\mathrm{o}} \quad L_{zz}^j = \frac{E_z(1-v_{r\theta}v_{\theta r})}{D_\mathrm{o}} \tag{4}$$

$$L_{r\theta}^j = \frac{E_r(v_{r\theta}-v_{rz}v_{z\theta})}{D_\mathrm{o}} = \frac{E_\theta(v_{\theta r}-v_{zr}v_{\theta z})}{D_\mathrm{o}} \tag{5}$$

$$L_{rz}^j = \frac{E_r(v_{rz}-v_{r\theta}v_{\theta z})}{D_\mathrm{o}} = \frac{E_z(v_{zr}-v_{\theta r}v_{\theta z})}{D_\mathrm{o}} \tag{6}$$

$$L_{\theta z}^j = \frac{E_\theta(v_{\theta z}-v_{\theta r}v_{rz})}{D_\mathrm{o}} = \frac{E_z(v_{z\theta}-v_{zr}v_{r\theta})}{D_\mathrm{o}} \tag{7}$$

where $D_\mathrm{o} = [1-(v_{r\theta}v_{\theta r}+v_{rz}v_{zr}+v_{\theta z}v_{z\theta})-(v_{r\theta}v_{\theta z}v_{zr}+v_{\theta r}v_{z\theta}v_{rz})]$, in terms of the elastic constants in (2), with the subscript (j) omitted.

Specific magnitudes of the above elastic constants can be derived by identifying the cylinder wall with a laminated plate of the same layup. The plate moduli are found from the classical laminated plate theory and are then transformed into cylindrical coordinates. This has been described in detail by Sun and Li (1988) and Luo and Sun (1991).

3. Fields in a single layer

Consider any single cylindrically orthotropic layer (j) that has been separated from the composite cylinder and constrained by prescribed uniform surface displacements,

$$u_r^j = u_a^j \quad \text{at } r = a_j, \quad u_r^j = u_b^j \quad \text{at } r = b_j, \quad u_z^j = \varepsilon_{zz}^j L \quad \text{at } z = L \tag{8}$$

In addition, certain uniform eigenstrains $\boldsymbol{\mu}_j = [\mu_{rr}^j \quad \mu_{\theta\theta}^j \quad \mu_{zz}^j]^T$ are prescribed in the layer. Our objective is to find the local strain and stress fields, and to relate the applied displacements and eigenstrains to the resulting tractions.

The kinematic relations for total strains $\boldsymbol{\varepsilon}^j$ and displacements $\boldsymbol{u}^j$ in the layer are,

$$\varepsilon_{rr} = \frac{\partial u_r^j}{\partial r} \quad \varepsilon_{\theta\theta} = \frac{u_r^j}{r} \quad \varepsilon_{zz}^j = \frac{u_z^j}{z} = \text{const} \quad \varepsilon_{r\theta}^j = \varepsilon_{zr}^j = \varepsilon_{z\theta}^j = 0 \tag{9}$$

The stresses then follow from eqn (3) and must satisfy the equations of equilibrium in cylindrical coordinates, which for zero body forces reduce to the single equation,

$$\frac{\sigma^j_{rr}-\sigma^j_{\theta\theta}}{r}+\frac{\partial\sigma^j_{rr}}{\partial r}=0 \tag{10}$$

the other equations are satisfied identically. Substituting (8) into (10), we find,

$$\frac{\partial^2 u^j_r}{\partial r^2}+\frac{1}{r}\frac{\partial u^j_r}{\partial r}-k^2_j\frac{u^j_r}{r^2}=\frac{1}{rL^j_{rr}}[(L^j_{rr}-L^j_{r\theta})\mu^j_{rr}+(L^j_{r\theta}-L^j_{\theta\theta})\mu^j_{\theta\theta}+(L^j_{rz}-L^j_{\theta z})(\mu^j_{zz}-\varepsilon^j_{zz})] \tag{11}$$

where $k^2_j = L^j_{\theta\theta}/L^j_{rr}$. In the particular case of a cylindrically orthotropic layer, it follows from eqn (3) that $k^2_j = E_\theta(1-\nu_{rz}\nu_{zr})/[E_r(1-\nu_{\theta z}\nu_{z\theta})]$.

The general solution of (11) can be found in the form,

$$u^j_r(\xi_j) = A_j b_j \xi_j^{k_j}+B_j b_j \xi_j^{-k_j}+u^\mu_r(\xi_j) \tag{12}$$

where $\xi_j = r/b_j$, b_j is the outer radius of the layer (j), and u^μ_r is a particular integral entirely dependent on the applied eigenstrains and the constant axial strain ε^j_{zz}. Two different particular integrals are found, according to the magnitude of $k^2_j = L^j_{\theta\theta}/L^j_{rr}$.

For $k_j \neq 1$ there is,

$$u^\mu_r(\xi_j) = b_j\xi_j S_j \quad S_j = [\mathscr{U}_j\mu^j_{rr}+\mathscr{B}_j\mu^j_{\theta\theta}-\mathscr{C}_j(\varepsilon^j_{zz}-\mu^j_{zz})] \tag{13}$$

and

$$\mathscr{U}_j = \frac{L^j_{rr}-L^j_{r\theta}}{L^j_{rr}(1-k^2_j)} = \frac{L^j_{rr}-L^j_{r\theta}}{L^j_{rr}-L^j_{\theta\theta}} \qquad \mathscr{B}_j = \frac{L^j_{r\theta}-L^j_{\theta\theta}}{L^j_{rr}(1-k^2_j)} = \frac{L^j_{r\theta}-L^j_{\theta\theta}}{L^j_{rr}-L^j_{\theta\theta}}$$

$$\mathscr{C}_j = \frac{L^j_{rz}-L^j_{\theta z}}{L^j_{rr}(1-k^2_j)} = \frac{L^j_{rz}-L^j_{\theta z}}{L^j_{rr}-L^j_{\theta\theta}} \qquad \mathscr{U}_j+\mathscr{B}_j = 1$$

For $k_j = 1$, the particular integral becomes,

$$u^\mu_r(\xi_j) = b_j\xi_j[\log(b_j\xi_j)-\tfrac{1}{2}]T_j, \quad T_j = [\mathscr{E}_j(\mu^j_{rr}-\mu^j_{\theta\theta})-\mathscr{F}_j(\varepsilon^j_{zz}-\mu^j_{zz})] \tag{14}$$

and

$$\mathscr{E}_j = \frac{L^j_{rr}-L^j_{r\theta}}{2L^j_{rr}} \qquad \mathscr{F}_j = \frac{L^j_{rz}-L^j_{\theta z}}{2L^j_{rr}}$$

Note that radially variable displacements are caused by the uniform eigenstrains in a fully constrained cylindrical layer, with the boundary conditions (8) prescribed as $u^j_a = u^j_b = u^j_z = 0$ in (13) or (14).

The integration constants in (12) are found from the boundary conditions (8). For $k_j \neq 1$, with $c_j = a_j/b_j$,

$$(1-c_j^{2k_j})A_j = -\frac{u_a^j}{a_j}c_j^{k_j+1} + \frac{u_b^j}{b_j} + S_j(c_j^{k_j+1}-1) \tag{15}$$

$$(1-c_j^{2k_j})B_j = \frac{u_a^j}{a_j}c_j^{k_j+1} - \frac{u_b^j}{b_j}c_j^{2k_j} + S_j(c_j^{2k_j}-c_j^{k_j+1}) \tag{16}$$

For $k_j = 1$,

$$(1-c_j^2)A_j = -\frac{u_a^j}{a_j}c_j^2 + \frac{u_b^j}{b_j} + T_j\left[c_j^2\log(a_j) - \log(b_j) + \frac{(1-c_j^2)}{2}\right] \tag{17}$$

$$(1-c_j^2)B_j = \left[\frac{u_a^j}{a_j} - \frac{u_b^j}{b_j}\right]c_j^2 - T_j c_j^2 \log c_j \tag{18}$$

The total strains are now found from (9) and the local stresses from (3), in terms of the loadings, u_a^j and u_b^j, $(\mu_{rr}^j - \mu_{\theta\theta}^j)$, and $(\varepsilon_{zz}^j - \mu_{zz}^j)$.

For $k_j \neq 1$,

$$\sigma_{rr}^j = A_j(L_{rr}^j k_j + L_{r\theta}^j)\xi_j^{k_j-1} - B_j(L_{rr}^j k_j - L_{r\theta}^j)\xi_j^{-k_j-1} + \Psi^j(\mu_{rr}^j - \mu_{\theta\theta}^j) + [-(L_{rr}^j + L_{r\theta})\mathscr{C}_j + L_{rz}^j](\varepsilon_{zz}^j - \mu_{zz}^j) \tag{19}$$

$$\sigma_{\theta\theta}^j = A_j(L_{r\theta}^j k_j + L_{\theta\theta}^j)\xi_j^{k_j-1} - B_j(L_{r\theta}^j k_j - L_{\theta\theta}^j)\xi_j^{-k_j-1} + \Psi^j(\mu_{rr}^j - \mu_{\theta\theta}^j) + [-(L_{r\theta}^j + L_{\theta\theta}^j)\mathscr{C}_j + L_{\theta z}^j](\varepsilon_{zz}^j - \mu_{zz}^j) \tag{20}$$

$$\sigma_{zz}^j = A_j(L_{rz}^j k_j + L_{\theta z}^j)\xi_j^{k_j-1} - B_j(L_{rz}^j k_j - L_{\theta z}^j)\xi_j^{-k_j-1} + (L_{rz}^j\mathscr{B}_j - L_{\theta z}^j\mathscr{U}_j)(\mu_{rr}^j - \mu_{\theta\theta}^j) + [-(L_{rz}^j + L_{\theta z})\mathscr{C}_j + L_{zz}^j](\varepsilon_{zz}^j - \mu_{zz}^j) \tag{21}$$

with the notation in (13), and $\Psi^j = -((L_{r\theta}^j)^2 - L_{rr}^j L_{\theta\theta}^j)/(L_{rr}^j - L_{\theta\theta}^j)$.

For $k_j = 1$

$$\sigma_{rr}^j = A_j(L_{rr}^j + L_{r\theta}^j) - B_j(L_{rr}^j - L_{r\theta}^j)\xi_j^{-2} + \Psi_1^j \log(b_j\xi_j)(\mu_{rr}^j - \mu_{\theta\theta}^j) + \Psi_2^j\mu_{rr}^j + \Psi_3^j\mu_{\theta\theta}^j + [\Phi_1^j\log(b_j\xi_j) + \Phi_2^j](\varepsilon_{zz}^j - \mu_{zz}^j) \tag{22}$$

$$\sigma_{\theta\theta}^j = A_j(L_{r\theta}^j + L_{rr}^j) - B_j(L_{rr}^j - L_{r\theta}^j)\xi_j^{-2} + \Psi_1^j \log(b_j\xi_j)(\mu_{rr}^j - \mu_{\theta\theta}^j) + \Psi_3^j\mu_{rr}^j + \Psi_2^j\mu_{\theta\theta}^j + [\Phi_1^j\log(b_j\xi_j) + \Phi_3^j](\varepsilon_{zz}^j - \mu_{zz}^j) \tag{23}$$

$$\sigma_{zz}^j = A_j(L_{rz}^j + L_{\theta z}^j) - B_j(L_{rz}^j - L_{\theta z}^j)\xi_j^{-2} + \Psi_4^j \log(b_j\xi_j)(\mu_{rr}^j - \mu_{\theta\theta}^j) + \Psi_5^j\mu_{rr}^j + \Psi_6^j\mu_{\theta\theta}^j + [\Phi_4^j\log(b_j\xi_j) + \Phi_5^j](\varepsilon_{zz}^j - \mu_{zz}^j) \tag{24}$$

where

$$\begin{aligned}
\Psi_1^j &= \mathscr{E}_j(L_{rr}^j + L_{r\theta}^j) & \Phi_1^j &= -\mathscr{F}_j(L_{rr}^j + L_{r\theta}^j) \\
\Psi_2^j &= \frac{\mathscr{E}_j(L_{rr}^j - L_{r\theta}^j)}{2} - L_{rr}^j & \Phi_2^j &= -\frac{\mathscr{F}_j(L_{rr}^j - L_{r\theta}^j)}{2} + L_{rz}^j \\
\Psi_3^j &= -\frac{\mathscr{E}_j(L_{rr}^j - L_{r\theta}^j)}{2} - L_{r\theta}^j & \Phi_3^j &= \frac{\mathscr{F}_j(L_{rr}^j - L_{r\theta}^j)}{2} + L_{\theta z}^j \\
\Psi_4^j &= \mathscr{E}_j(L_{rz}^j + L_{\theta z}^j) & \Phi_4^j &= -\mathscr{F}_j(L_{rz}^j + L_{\theta z}^j) \\
\Psi_5^j &= \frac{\mathscr{E}_j(L_{rz}^j - L_{\theta z}^j)}{2} - L_{rz}^j & \Phi_5^j &= -\frac{\mathscr{F}_j(L_{rz}^j - L_{\theta z}^j)}{2} + L_{zz}^j \\
\Psi_6^j &= -\frac{\mathscr{E}_j(L_{rz}^j - L_{\theta z}^j)}{2} - L_{\theta z}^j
\end{aligned} \tag{25}$$

The average values of the stress components through the thickness of the layer are defined as

$$\langle \sigma_{pp}^j \rangle = \frac{1}{(b_j - a_j)} \int_{a_j}^{b_j} \sigma_{pp}^j \, \mathrm{d}r \quad \langle \sigma_{zz}^j \rangle = \frac{1}{V_j} \int_{V_j} \sigma_{zz}^j \, \mathrm{d}V_j \tag{26}$$

for $p = r$ and $p = \theta$; $(b_j - a_j)$ is the thickness and $V_j = \pi(b_j^2 - a_j^2)$ is the volume of a unit length of the j-th layer. Moreover, we define at the boundary of the layer

$$P_a^j = -(p_a^j a_j) \quad P_b^j = (p_b^j b_j) \quad P_z^j = \langle \sigma_{zz}^j \rangle V_j \tag{27}$$

where $p_a^j = \sigma_{rr}^j$ at $r = a_j$, and $p_b^j = \sigma_{rr}^j$ at $r = b_j$, and write the force–displacement relation for a single layer (j) under the boundary conditions (8) and the eigenstrains $\boldsymbol{\mu}_j$ as,

$$\begin{Bmatrix} P_a^j \\ P_b^j \\ P_z^j \end{Bmatrix} = \boldsymbol{k}^j \begin{Bmatrix} u_a^j \\ u_b^j \\ u_z^j \end{Bmatrix} + \boldsymbol{q}^j \begin{Bmatrix} \mu_{rr}^j \\ \mu_{\theta\theta}^j \\ \mu_{zz}^j \end{Bmatrix} \tag{28}$$

where the coefficients $\boldsymbol{k}^j$ and $\boldsymbol{q}^j$ are evaluated from (19)–(21) and (26), (27) for $k_j \neq 1$, or from (22)–(24) and (26), (27) for $k_j = 1$. Results appear in the Appendix.

Applying the averages (26) to the stress fields (19)–(21) or (22)–(24), we find,

$$\begin{Bmatrix} \langle \sigma_{rr}^j \rangle \\ \langle \sigma_{\theta\theta}^j \rangle \\ \langle \sigma_{zz}^j \rangle \end{Bmatrix} = \boldsymbol{s}^j \begin{Bmatrix} u_a^j \\ u_b^j \\ u_z^j \end{Bmatrix} + \boldsymbol{w}^j \begin{Bmatrix} \mu_{rr}^j \\ \mu_{\theta\theta}^j \\ \mu_{zz}^j \end{Bmatrix} \tag{29}$$

Also, we define eigenstresses $\boldsymbol{\lambda}^j$ as the average stresses caused in a fully constrained layer, $\boldsymbol{u}^j = \boldsymbol{0}$, by the uniform eigenstrains $\boldsymbol{\mu}^j$,

$$\boldsymbol{\lambda}^j = \boldsymbol{w}^j \boldsymbol{\mu}^j \tag{30}$$

This is not necessarily identical with the definition $\boldsymbol{\lambda} = -\boldsymbol{L}\boldsymbol{\mu}$, usually adopted in the Cartesian system, where the stresses caused by uniform eigenstrains in a fully constrained homogeneous volume are also known. The coefficients of $\boldsymbol{w}^j$ also appear in the Appendix.

4. Overall response of the cylindrical structure

We now proceed to find expressions for the local stresses in the layers and for the overall response of the cylindrical composite structure under loads consisting of an external pressure p_b at the external boundary $r = b$ and $z = 0$, L, certain pressure p_a at the internal boundary $r = a$, and uniform eigenstrains $\boldsymbol{\mu}^p$ prescribed in selected layers $j = p$. In general, the tractions at the respective surfaces are defined in analogy with (27) as,

$$P_a = P_a^1 = -(p_a^1 a) \quad P_b = P_b^N = (p_b^N b) \quad P_z = \sum_{i=1}^{N} P_z^i = \sum_{i=1}^{N} \langle \sigma_{zz}^i \rangle V_i \tag{31}$$

where $i = 1, 2, \ldots, N$, and the last equality reflects force equilibrium in the axial direction. Two types of eigenstrains are admitted in the layers, fixed eigenstrains $\bar{\boldsymbol{\mu}}^i$ and variable eigenstrains $\boldsymbol{\mu}^j$ $(i, j = 1, 2, \ldots, N)$ that can be adjusted in fabrication or service in order to achieve a certain optimum distribution of internal stresses under the external loads (31). In any case, the eigenstrains are first converted into internal tractions by referring to (28) and letting all surface displacements vanish. These tractions are then applied to the structure, with reversed signs, as internal line tractions on layer interfaces and at the external boundaries of the surface layers; their evaluation is,

$$\begin{Bmatrix} \bar{F}_a^i \\ \bar{F}_b^i \\ \bar{F}_z^i \end{Bmatrix} = -\boldsymbol{q}^i \begin{Bmatrix} \bar{\mu}_{rr}^i \\ \bar{\mu}_{\theta\theta}^i \\ \bar{\mu}_{zz}^i \end{Bmatrix} \qquad \begin{Bmatrix} F_a^i \\ F_b^i \\ F_z^i \end{Bmatrix} = -\boldsymbol{q}^i \begin{Bmatrix} \mu_{rr}^i \\ \mu_{\theta\theta}^i \\ \mu_{zz}^i \end{Bmatrix} \tag{32}$$

As in $(31)_3$, the total axial tractions acting on the structure are,

$$\bar{F}_z = \sum_{i=1}^{N} \bar{F}_z^i \qquad F_z = \sum_{j=1}^{N} F_z^j \tag{33}$$

The solution is sought for the loads (31) and (32), in terms of the radial displacements at the layer interfaces; once these are known, the internal stresses in the layers can be found from (19)–(24). The interface radial displacement components must satisfy,

$$u^1 = u_a \quad \text{at} \quad r = a, \quad u^i = u_a^i = u_b^{i-1} \quad \text{at} \quad r = a_i = b_{i-1}, \quad u^{N+1} = u_b^N \quad \text{at} \quad r = b \tag{34}$$

and the axial displacements the condition $u_z^i = u_z$. The total tractions caused on the interfaces by the mechanical loads (31) and by the eigenstrain-generated tractions (32) must be in equilibrium, so that,

$$P^1 = P_a \quad \text{at} \quad r = a, \quad P^i = P_a^i = P_b^{i-1} \quad \text{at} \quad r = a_i = b_{i-1}, \quad P^{N+1} = P_b^N \quad \text{at} \quad r = b \tag{35}$$

Subject to these conditions, and to the equilibrium requirements $(31)_3$ and (33), the interface displacements are found from,

$$\boldsymbol{K}\begin{Bmatrix} u^1 \\ u^2 \\ \vdots \\ u^j \\ u^{j+1} \\ \vdots \\ u^N \\ u^{N+1} \\ u_z \end{Bmatrix} = \begin{Bmatrix} P_a \\ 0 \\ \vdots \\ 0 \\ 0 \\ \vdots \\ 0 \\ P_b \\ P_z \end{Bmatrix} + \begin{Bmatrix} \bar{F}_a^1 \\ \bar{F}_a^2+\bar{F}_b^1 \\ \vdots \\ \bar{F}_a^j+\bar{F}_b^{j-1} \\ \bar{F}_a^{j+1}+\bar{F}_b^j \\ \vdots \\ \bar{F}_a^N+\bar{F}_b^{N-1} \\ \bar{F}_b^N \\ \bar{F}_z \end{Bmatrix} + \sum_{j\in J}\begin{Bmatrix} 0 \\ 0 \\ \vdots \\ F_a^j \\ F_b^j \\ \vdots \\ 0 \\ 0 \\ F_z^j \end{Bmatrix} \begin{matrix} \\ \\ \\ j\text{-th position} \\ j+1\text{-th position} \\ \\ \\ \\ \\ \end{matrix} \tag{36}$$

or, from,

$$\boldsymbol{Ku} = \boldsymbol{P}+\bar{\boldsymbol{F}}+\sum_{j\in J}\boldsymbol{F}^j \tag{37}$$

where J denotes the set of layers which contain the adjustable eigenstrains $\boldsymbol{\mu}^j$.

The stiffness matrix $\boldsymbol{K}$ of the cylindrical structure can be written in terms of the layer stiffness coefficients k^i_{mn} defined in (28) and listed in the Appendix,

$$\boldsymbol{K} = \begin{bmatrix} k^1_{11} & k^1_{12} & 0 & \dots & 0 & 0 & k^1_{13} \\ k^1_{12} & k^2_{11}+k^1_{22} & k^2_{12} & \dots & 0 & 0 & k^2_{13}+k^1_{23} \\ 0 & k^2_{12} & k^3_{11}+k^2_{22} & \dots & 0 & 0 & k^3_{13}+k^2_{23} \\ \vdots & \vdots & \vdots & \ddots & \vdots & \vdots & \vdots \\ 0 & 0 & 0 & \dots & k^N_{11}+k^{N-1}_{22} & k^{N-1}_{12} & k^N_{13}+k^{N-1}_{23} \\ 0 & 0 & 0 & \dots & k^{N-1}_{12} & k^N_{22} & k^N_{23} \\ k^N_{31} & k^2_{31}+k^1_{32} & k^3_{31}+k^2_{32} & \dots & k^N_{31}+k^{N-1}_{32} & k^N_{32} & \Sigma^N_{\alpha=1}k^\alpha_{33} \end{bmatrix} \tag{38}$$

Note that $\boldsymbol{K}$ is neither symmetric nor banded. On the other hand, if $\boldsymbol{K}$ is partitioned as

$$\boldsymbol{K} = \begin{bmatrix} \boldsymbol{K}_{11\{(N+1)\times(N+1)\}} & \boldsymbol{K}_{12\{(N+1)\times 1\}} \\ \boldsymbol{K}_{21\{1\times(N+1)\}} & K_{22\{1\times 1\}} \end{bmatrix} \tag{39}$$

the matrix $\boldsymbol{K}_{11}$ is symmetric, positive definite, tridiagonal and banded.

The solution of (36) or (37) is thus sought as a superposition of two problems denoted as (I) and (II). First, a plane strain problem ($u_z = 0$) is solved under the prescribed tractions P_a and P_b in (31), and for the eigenstrain-generated tractions (32). Then, the cylinder structure is freed of any overall constraints and subjected to the applied axial forces, and to such forces that remove the axial reactions found in the plane strain solution. Thus (37) is rewritten as,

$$\begin{bmatrix} \boldsymbol{K}_{11} & \boldsymbol{K}_{12} \\ \boldsymbol{K}_{21} & K_{22} \end{bmatrix}\begin{Bmatrix} \boldsymbol{u} \\ u_z \end{Bmatrix} = \bar{\boldsymbol{F}}^r+\bar{\boldsymbol{F}}^z+\boldsymbol{P}_z+\sum_{j\in J}(\boldsymbol{F}^r_j+\boldsymbol{F}^z_j) \tag{40}$$

where we defined the $\{(N+2)\times 1\}$ matrices as,

$$\bar{\boldsymbol{F}}^r = \begin{Bmatrix} P_a + \bar{F}_a^1 \\ \bar{F}_a^2 + \bar{F}_b^1 \\ \vdots \\ \bar{F}_a^j + \bar{F}_b^{j-1} \\ \bar{F}_a^{j+1} + \bar{F}_b^j \\ \vdots \\ \bar{F}_a^N + \bar{F}_b^{N-1} \\ \bar{F}_b^N + P_b \\ \bar{R}_z \end{Bmatrix} \tag{41}$$

$$\bar{\boldsymbol{F}}_z = (0 \quad 0 \quad \ldots \quad 0 \quad 0 \quad \ldots \quad 0 \quad 0 \quad -\bar{R}_z + \bar{F}_z)^T \tag{42}$$

$$\boldsymbol{P}_z = (0 \quad 0 \quad \ldots \quad 0 \quad 0 \quad \ldots \quad 0 \quad 0 \quad P_z)^T \tag{43}$$

$$\boldsymbol{F}_j^r = (0 \quad 0 \quad \ldots \quad 0 \quad 0 \quad \ldots \quad 0 \quad 0 \quad R_z^j)^T \tag{44}$$

$$\boldsymbol{F}_j^z = (0 \quad 0 \quad \ldots \quad 0 \quad 0 \quad \ldots \quad 0 \quad 0 \quad -R_z^j + F_z^j)^T \tag{45}$$

In the first, plane strain part (I) of the solution, the structure is loaded by $\bar{\boldsymbol{F}}^r$ and $\Sigma\bar{\boldsymbol{F}}_j^r$ in (40). The two loads are applied separately and the resulting radial displacements are then added as $\boldsymbol{u}^{\mathrm{I}} = \bar{\boldsymbol{u}}^{\mathrm{I}} + \boldsymbol{u}_j^{\mathrm{I}}$. The first system to be solved is written for the $(N+1)$ radial displacements,

$$\boldsymbol{K}_{11}\bar{\boldsymbol{u}}^{\mathrm{I}} = \bar{\boldsymbol{F}}^r \quad \text{and} \quad \boldsymbol{K}_{11}\boldsymbol{u}_j^{\mathrm{I}} = \bar{\boldsymbol{F}}_j^r \quad j \in J \tag{46}$$

where J denotes the set of layers with nonzero eigenstrains, and where only the first $(N+1)$ coefficients of $\bar{\boldsymbol{F}}^r$ and $\boldsymbol{F}_j^r$ are actually used. The as yet unknown axial reactions then are,

$$\bar{R}_z = \boldsymbol{K}_{21}\bar{\boldsymbol{u}}^{\mathrm{I}} \quad R_z^j = \boldsymbol{K}_{21}\boldsymbol{u}_j^{\mathrm{I}} \quad j \in J \tag{47}$$

and the components $\bar{\boldsymbol{F}}_z$ and $\boldsymbol{F}_j^z$ follow directly from (32). This provides complete information about the axial loading vectors $\bar{\boldsymbol{F}}^z$ and $\Sigma\boldsymbol{F}_z^j$ in (40); $\boldsymbol{P}_z$ is the prescribed load.

In the second part (II) of the solution, the structure is loaded only by the load vector that represents the total axial force,

$$\boldsymbol{R} = \bar{\boldsymbol{F}}^z + \boldsymbol{P}^z + \sum_{j \in J} \boldsymbol{F}_j^z \tag{48}$$

To evaluate the local radial displacements $\boldsymbol{u}^{\mathrm{II}}$ at the layer interfaces and the axial displacement u_z^{II}, we first find $\boldsymbol{u} = \boldsymbol{u}^\circ$ for a certain axial displacement, say for $u_z^\circ = 1$. According to (40), this follows from the relation,

$$\boldsymbol{K}_{11}\boldsymbol{u}^\circ = -\boldsymbol{K}_{12}u_z^\circ \tag{49}$$

and the axial reaction corresponding to the selected u_z° is,

$$R^\circ = \boldsymbol{K}_{21}\boldsymbol{u}^\circ + K_{22}u_z^\circ = (K_{22} - \boldsymbol{K}_{21}\boldsymbol{K}_{11}^{-1}\boldsymbol{K}_{12})u_z^\circ \tag{50}$$

Equation (40) indicates that the total axial force $\boldsymbol{R}$ in (48) has the single nonzero component,

$$R = -R_z + \bar{F}_z + P_z - R_z^j + \sum_{j\in J} F_j^z \tag{51}$$

Using this value to replace R° in (50), we find the actual axial displacement for the second part (II) of the superposition. Since we selected $u_z^{\mathrm{I}} = 0$, the total u_z in (40) is

$$u_z = u_z^{\mathrm{II}} = (K_{22} - \boldsymbol{K}_{21}\boldsymbol{K}_{11}^{-1}\boldsymbol{K}_{12})^{-1}\left(-R_z + \bar{F}^z + P_z - R_z^j + \sum_{j\in J} F_j^z\right) \tag{52}$$

where the forces are evaluated from (32) and (47). Then, a substitution into (49) provides the radial displacements due to the actual axial force R as,

$$\boldsymbol{u}^{\mathrm{II}} = -\boldsymbol{K}_{11}^{-1}\boldsymbol{K}_{12}(K_{22} - \boldsymbol{K}_{21}\boldsymbol{K}_{11}^{-1}\boldsymbol{K}_{12})^{-1}\left(-R_z + \bar{F}^z + P_z - R_z^j + \sum_{j\in J} F_j^z\right) \tag{53}$$

Finally, we recall from (46) the radial displacements in the plane strain problem (I)

$$\boldsymbol{u}^{\mathrm{I}} = \bar{\boldsymbol{u}}^{\mathrm{I}} + \boldsymbol{u}_j^{\mathrm{I}} = \boldsymbol{K}_{11}^{-1}(\bar{\boldsymbol{F}}^r + \bar{\boldsymbol{F}}_j^r) \tag{54}$$

and invoke the superposition $\boldsymbol{u} = \boldsymbol{u}^{\mathrm{I}} + \boldsymbol{u}^{\mathrm{II}}$ to complete the solution of (40). Note that the solution calls only for the evaluation of $\boldsymbol{K}_{11}^{-1}$, which is asymmetric and positive definite matrix, so that the inverse can be found using the Choleski decomposition.

5. Transformation influence functions

We now proceed to derive certain influence functions that evaluate the effect of unit uniform eigenstrains introduced in one layer $j = p$ on the stress fields in all layers. In this derivation, all other layers ($i \neq p$) are assumed to be free of initial strains.

Suppose that a single layer ($j \in J$) is subjected to a uniform eigenstrain $\boldsymbol{\mu} = \{\mu_{rr}^j, \mu_{\theta\theta}^j, \mu_{zz}^j\}$ of unit magnitude. As pointed out in Section 4, the effect of this eigenstrain on the layered cylindrical structure can be represented by application of interface tractions $\boldsymbol{F}^j$ given by $(32)_2$, as $r = a_j$ and $r = b_j$. The displacements $\boldsymbol{u}$ at all interfaces between the layers then follow from (37) for $\boldsymbol{P} = \bar{\boldsymbol{F}} = \boldsymbol{0}$ as,

$$\boldsymbol{K}\boldsymbol{u} = \boldsymbol{F}^j \tag{55}$$

The form of $\boldsymbol{F}^j$ required in (36) or (37) is written as,

$$\boldsymbol{F}^j = -\boldsymbol{Q}^j\boldsymbol{\mu}^j \tag{56}$$

where the coefficients of $\boldsymbol{Q}^j$ are taken from (32) and arranged as follows,

$$\boldsymbol{Q}^j = \left\{\begin{matrix} 0 & 0 & 0 \\ 0 & 0 & 0 \\ \vdots & \vdots & \vdots \\ q_{11} & q_{12} & q_{13} \\ q_{21} & q_{22} & q_{23} \\ \vdots & \vdots & \vdots \\ 0 & 0 & 0 \\ \vdots & \vdots & \vdots \\ q_{31} & q_{32} & q_{33} \end{matrix}\right\} \begin{matrix} j\text{-th position} \\ j+1\text{-th position} \end{matrix} \tag{57}$$

Next, we extract the (3×1) displacement vector $\bar{\boldsymbol{u}}^i = \{u_a^i, u_b^i, u_z^i\}$ for a specific layer $i = 1, 2, , \ldots, N$ from the $((N+2)\times 1)$ vector $\boldsymbol{u}$ of all radial displacements in the structure,

$$\bar{\boldsymbol{u}}^i = \begin{Bmatrix} u_a^i \\ u_b^i \\ u_z^i \end{Bmatrix} = \begin{bmatrix} 0 & 0 & 0 & \ldots & 0 & 1 & 0 & 0 & \ldots & 0 \\ 0 & 0 & 0 & \ldots & 0 & 0 & 1 & 0 & \ldots & 0 \\ 0 & 0 & 0 & \ldots & 0 & 0 & 0 & 0 & \ldots & 1 \\ & & & & & \underbrace{}_{i\text{-th position}} & \underbrace{}_{i+1\text{-th position}} & & & \end{bmatrix} \boldsymbol{u} = \boldsymbol{H}_i \boldsymbol{u}. \tag{58}$$

Thus we find the solution of (55) in the form,

$$\bar{\boldsymbol{u}}^i = -\boldsymbol{H}_i \boldsymbol{K}^{-1} \boldsymbol{Q}^j \boldsymbol{\mu}^j, \tag{59}$$

which evaluates the displacements caused at the interfaces and in the axial direction of any layer (i) by the uniform eigenstrains applied in the layer (j); it includes the self-induced displacements in the layer ($i = j$).

Of course, our goal is to find the local stresses $\boldsymbol{\sigma}^i$ caused by the eigenstrain $\boldsymbol{\mu}^j$. This is accomplished by substituting from (59) into (29). Rewriting (29) as

$$\begin{aligned} \langle \boldsymbol{\sigma}^j \rangle &= \boldsymbol{s}^j \bar{\boldsymbol{u}}^j + \boldsymbol{w}^j \boldsymbol{\mu}^j \quad \text{for } i = j \\ \langle \boldsymbol{\sigma}^i \rangle &= \boldsymbol{s}^i \bar{\boldsymbol{u}}^i \quad \text{for } i \neq j \end{aligned} \tag{60}$$

and taking $\bar{\boldsymbol{u}}^i$ from (59) and $\boldsymbol{\mu}^j$ from (30), we find,

$$\langle \boldsymbol{\sigma}^i \rangle = [\delta_{ij} \boldsymbol{I}_3 - \boldsymbol{s}^i \boldsymbol{H}_i \boldsymbol{K}^{-1} \boldsymbol{Q}^j (\boldsymbol{w}^j)^{-1}] \boldsymbol{\lambda}^j = \boldsymbol{F}_{ij} \boldsymbol{\lambda}^j \tag{61}$$

where $i,j = 1, 2, \ldots, N$, δ_{ij} is the Kronecker symbol but the summation rule is not observed, $\boldsymbol{I}_3$ is a (3×3) unit matrix, and $\boldsymbol{w}^j$ is defined in (29). One can show that $\det|\boldsymbol{w}^j| \neq 0$.

Another useful form relates to the layer eigenstrains and local stresses as,

$$\langle \boldsymbol{\sigma}^i \rangle = \boldsymbol{D}_{ij} \boldsymbol{\mu}^j \qquad \boldsymbol{D}_{ij} = \boldsymbol{F}_{ij} \boldsymbol{w}^j \qquad i,j = 1, 2, \ldots, N \tag{62}$$

The $\boldsymbol{D}_{ij}$ and $\boldsymbol{F}_{ij}$ are the eigenstrain and eigenstress influence functions, that evaluate residual stresses in the layered cylinder due to unit transformations induced in layer (j), analogous to those introduced in Dvorak and Benveniste (1992) and Dvorak (1992).

We note that (61) can be readily used for evaluation of layer stresses caused by known eigenstrains, such as thermal strains or moisture-induced swelling. In particular, the linear thermal expansion coefficients of the layer material are multiplied by the temperature difference $T-T_c$ between the current and curing temperature, and identified with the layer eigenstrains in (1). These thermally-induced layer eigenstrains are regarded as fixed, denoted by $\bar{\boldsymbol{\mu}}^i$, used in $(32)_1$ to find the corresponding internal tractions $\bar{\boldsymbol{F}}$ that appear in (36). The moisture-induced eigenstrains are treated in a similar way, but with expansion coefficients and moisture content data. The average layer stresses are then given by (61) and (62).

6. Design of laminate layup

Stresses generated by the external hydrostatic pressure are often of primary concern in design of submerged structures. In the thin-walled ($D/t > 20$) composite cylinder of diameter D and wall thickness t, the average stresses in the cylinder wall in the axial, hoop and radial directions, Fig. 1, evaluate as,

$$\sigma_z = p\left(\frac{D}{4t}\right) \qquad \sigma_\theta = p\left(\frac{D}{2t}\right) = 2\sigma_z \qquad 0 > \sigma_r > p \tag{63}$$

where $p < 0.2\sigma_z < 0$ denotes the applied external pressure. The radial compressive stress σ_r is small; as shown in Section 7 below, it is much smaller than the transverse compressive strength of typical polymer matrix plies and thus of no concern in laminate design. However, the through-the-thickness compression does cause (tensile) in-plane strains in a ply,

$$\varepsilon_\alpha = -\left(\frac{v_A}{E_A}\right)\sigma_r \qquad \varepsilon_\beta = -\left(\frac{v_T}{E_T}\right)\sigma_r \qquad \varepsilon_\gamma = \left(\frac{1}{E_T}\right)\sigma_r \tag{64}$$

where x_α is parallel to the fiber direction, x_β is in the plane of the ply, and x_γ is perpendicular to the $x_\alpha x_\beta$-plane; E_A, E_T, v_A, v_T are axial and transverse Young′s moduli and Poisson′s ratios of the ply. A reasonably accurate approximation of the axial fiber stress is $\sigma_\alpha^f = E_A^f \varepsilon_\alpha = -(v_A E_A^f/E_A)\sigma_r$. This is tension, hence it provides a small benefit in the present context. Typical values in epoxy-matrix systems are $\sigma_\alpha^f \simeq 0.5\sigma_r$.

The principal design goal is to assure that the compressive stresses in all plies of the laminate are well within certain allowable limits. The axial elastic modulus of a composite ply is typically much larger than the transverse modulus, hence the external load is supported primarily by the axial compressive stresses in the plies. For best use of the composite material and minimum weight of the structure, the laminate layup should be designed such that the axial compressive stresses in all plies are of the same magnitude. This requirement is met by laminate layups that respond to the above proportional biaxial normal stresses by isotropic in-plane deformation. Symmetric laminates with orthotropic in-plane material symmetry are well suited for this purpose.

The design problem is posed as follows: For the above stress ratio $\sigma_z = 2\sigma_\theta$, identify laminate layups that respond by isotropic in-plane strains, $\varepsilon_z = \varepsilon_\theta$. The first task is to determine conditions for laminate stiffness coefficients that guarantee the desired response. Then, corresponding laminate layups need to be found for specific material systems.

Since the wall curvature is small, the in-plane properties of the laminates can be estimated by the classical laminated plate theory for in-plane loading, as in Section 2. Therefore, for greater clarity, the above design problem can be solved for an element of a symmetric, orthotropic laminated plate under in-plane normal stresses. As is customary in such situations, we utilize Cartesian coordinates x_i, $i = 1, 2, 3$ and identify the ply with the fibers parallel to the x_1-direction as the 0° ply. In the context of the cylindrical coordinates of Fig. 1, x_1 is parallel to the z-direction, x_2 to the θ-direction, and x_3 to the r-direction. Accordingly, the stresses in (63) are relabeled as,

$$\sigma_z = \sigma_1 = p\left(\frac{D}{4t}\right) \qquad \sigma_\theta = \sigma_2 = p\left(\frac{D}{2t}\right) = 2\sigma_z \tag{65}$$

Using standard contracted notation, the constitutive relations of the orthotropic laminate under plane stress can be written in the form (Christensen, 1979),

$$\begin{bmatrix}\sigma_1\\ \sigma_2\\ \sigma_6\end{bmatrix} = \begin{bmatrix} L_{11} & L_{12} & 0\\ & L_{22} & 0\\ \text{sym} & & L_{66}\end{bmatrix}\begin{bmatrix}\varepsilon_1\\ \varepsilon_2\\ \varepsilon_6\end{bmatrix} \tag{66}$$

In the absence of in-plane shear stress, this can be reduced to two equations for the strains, with the solution

$$\varepsilon_1 = \frac{(L_{22}\sigma_1 - L_{12}\sigma_2)}{(L_{11}L_{22} - L_{12}^2)} \qquad \varepsilon_2 = \frac{-(L_{12}\sigma_1 - L_{11}\sigma_2)}{(L_{11}L_{22} - L_{12}^2)} \tag{67}$$

Substitute now the above prescribed stresses and desired strains,

$$\sigma_2 = 2\sigma_1 \qquad \varepsilon_2 = \varepsilon_1 \tag{68}$$

and thus obtain,

$$\frac{\sigma_1(L_{22} - 2L_{12})}{(L_{11}L_{22} - L_{12}^2)} = \frac{\sigma_1(2L_{11} - L_{12})}{(L_{11}L_{22} - L_{12}^2)} \tag{69}$$

which suggests that the stiffness coefficients of the laminate must satisfy the condition,

$$L_{22} - 2L_{12} + L_{12} - 2L_{11} = 0 \quad \Rightarrow \quad 2L_{11} - L_{22} + L_{12} = 0 \tag{70}$$

Next, we proceed to identify laminate layups that satisfy (70) in a specific material system. Noting that a layup is defined both by layer orientation and by the volume fraction (t_i/t) of layers of a particular orientation, we derive expressions for the volume fractions of layers needed to satisfy the said condition for certain standard layer orientations.

First to be considered is the $(0_{c_0}/90_{c_{90}})_s$ laminate. The objective is to evaluate the volume fractions $c_0 + c_{90} = 1$. Recall that the laminate (3×3) in-plane stiffness (66) is,

$$\boldsymbol{L} = c_0 \boldsymbol{L}_0 + c_{90} \boldsymbol{L}_{90}$$

$$\begin{bmatrix} L_{11} & L_{12} & 0 \\ & L_{22} & 0 \\ \text{sym} & & L_{66} \end{bmatrix} = c_0 \begin{bmatrix} L_{11}^0 & L_{12}^0 & 0 \\ & L_{22}^0 & 0 \\ \text{sym} & & L_{66}^0 \end{bmatrix} + c_{90} \begin{bmatrix} L_{22}^0 & L_{12}^0 & 0 \\ & L_{11}^0 & 0 \\ \text{sym} & & L_{66}^0 \end{bmatrix} \tag{71}$$

where L_{ij}^0 are stiffness coefficients of the $0°$ ply. Substituting this into $2L_{11} - L_{22} + L_{12} = 0$, one finds that,

$$(2c_0 - c_{90}) L_{11}^0 - (c_0 - 2c_{90}) L_{22}^0 + L_{12}^0 = 0 \tag{72}$$

Since $c_{90} = 1 - c_0$, it follows that,

$$3c_0 (L_{11}^0 - L_{22}^0) - L_{11}^0 + 2L_{22}^0 + L_{12}^0 = 0 \qquad c_0 = \frac{(L_{11}^0 - 2L_{22}^0 - L_{12}^0)}{3(L_{11}^0 - L_{22}^0)} \tag{73}$$

$$c_{90} = 1 - c_0 = 1 - \frac{(L_{11}^0 - 2L_{22}^0 - L_{12}^0)}{3(L_{11}^0 - L_{22}^0)} \tag{74}$$

For plies made of a chosen composite system with in-plane stiffness $\boldsymbol{L}_0$, these ply volume fractions will assure satisfaction of the condition $2L_{11} - L_{22} + L_{12} = 0$ in (70), for laminate in-plane stiffness coefficients of the $(0_{c_0}/90_{c_{90}})_s$ laminate.

Examining the conditions $0 < c_0 < 1$ and $0 < c_{90} < 1$, we find from (73) and (74),

$$(L_{11}^0 - 2L_{22}^0 - L_{12}^0) < 3(L_{11}^0 - L_{22}^0) \Rightarrow 2L_{11}^0 - L_{22}^0 + L_{12}^0 > 0 \tag{75}$$

This form is coincidentally similar to (70); it is satisfied in typical polymer matrix systems. Therefore, one can conclude that for such typical systems, the ply volume fractions (74) will satisfy the requirements $0 < c_0 < 1$ and $0 < c_{90} < 1$.

For example, in a glass-epoxy system with the ply stiffness coefficients,

$$L_{11}^0 = 37.3 \text{ GPa} \quad L_{12}^0 = 2.5 \text{ GPa} \quad L_{22}^0 = 8.5 \text{ GPa} \quad c_0 = 0.206 \quad c_{90} = 0.794 \quad c_{90}/c_0 = 3.85$$

$$L_{11} = 14.3 \text{ GPa} \quad L_{22} = 31.0 \text{ GPa} \quad L_{22}/L_{11} = 2.16$$

Similar results are obtained for the AS4/3501-6 carbon-epoxy system,

$$c_{90}/c_0 = 3.15 \qquad L_{22}/L_{11} = 112.8/49.8 = 2.26$$

Consider next a balanced $(0_{c_0}/60_{c_{60}}/90_{c_{90}})_s$ laminate where the $+60$ and -60 plies come in pairs and the c_{60} designates the volume fraction of these pairs. Since three ply volume fractions will be needed here, we consider a specific composite system, a variant of the AS4/3501-6, with the following ply moduli:

$$E_A = 142 \text{ GPa}, \quad E_T = 10.3 \text{ GPa}, \quad G_A = 7.2 \text{ GPa}, \quad \nu_A = 0.28$$

The ply stiffness coefficients (in GPa) in laminate coordinates are found as,

Ply	L_{11}	L_{12}	L_{16}	L_{22}	L_{26}	L_{66}
0	142.8	2.8	0	10.4	0	7.2
+60	21.2	25.1	15.8	87.4	41.5	29.5
−60	21.2	25.1	−15.8	87.4	−41.5	29.5
90	10.4	2.8	0	142.8	0	7.2

The laminate stiffness coefficients are found from the formula

$$L_{ij} = c_0 L_{ij}^0 + \frac{c_{60}}{2}(L_{ij}^{+60} + L_{ij}^{-60}) + c_{90} L_{ij}^{90} \tag{76}$$

Where the L_{ij} are evaluated using the numerical magnitudes from the above table, and substituted in the condition for laminate stiffnesses $2L_{11} - L_{22} + L_{12} = 0$, one finds the relations for ply volume fractions,

$$277.95c_0 - 19.95c_{60} - 119.25c_{90} = 0 \qquad c_0 + c_{60} + c_{90} = 1$$

Solutions can be found as functions of a parameter, c_{60}, for example. The results are,

c_0	0.100	0.150	0.200	0.250	0.300
c_{60}	0.801	0.600	0.400	0.200	0.000
c_{90}	0.099	0.250	0.400	0.550	0.700
L_{11}	32.28	36.75	41.20	45.65	50.10
L_{12}	20.62	16.15	11.70	7.25	2.80
L_{22}	85.18	89.65	94.10	98.55	103.01
L_{66}	25.03	20.56	16.10	11.65	7.20

The final selection may depend on such factors as distribution of volume fractions among ply orientation, on the magnitudes of the stiffnesses, both in-plane and the L_{66} that resists torsion.

Figure 2 presents the design diagram of AS4/3501-6 system in $(0_{c_0}/\pm 45_{c_{45}}/90_{c_{90}})$ laminate configuration. The volume fraction c_{45} is selected as the variable on the horizontal axis, while all ply volume fractions are plotted on the left vertical axis and their change as a function of c_{45} is indicated by the corresponding lines. The range of the useful volume fractions is quite limited here. The changes in the four stiffness coefficients are measured on the right vertical scale, and indicated by the superimposed lines. Figure 3 shows analogous results, for the $(0_{c_0}/\pm 60_{c_{60}}/90_{c_{90}})$ laminate whose tabulated results are given above. The c_{60} volume fraction of the pairs of ± 60 plies is used as a variable on the horizontal axis, and the two vertical axes serve the same purpose as in Fig. 2. The range of useful ply volume fractions is much wider for this laminate.

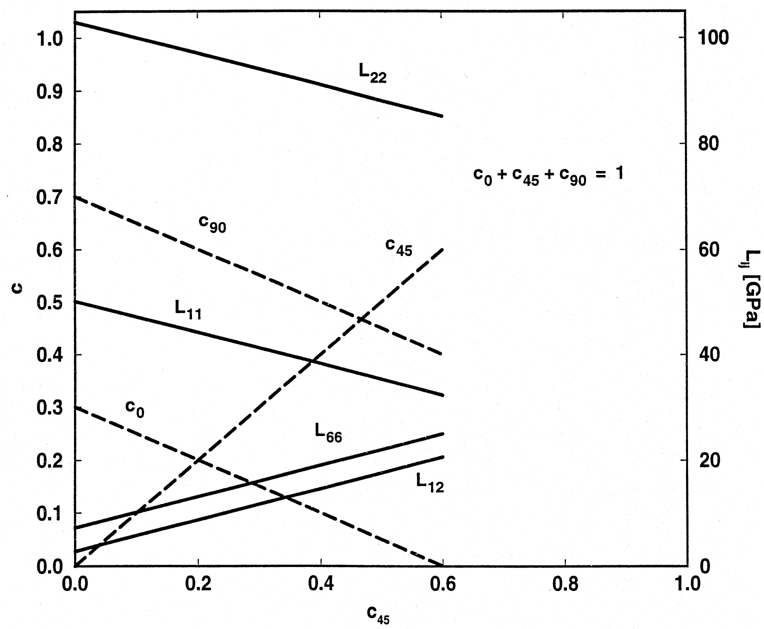

Fig. 2. Design diagram for a $(0_{c_0}/45_{c_{45}}/90_{c_{90}})$, AS4/3501-6 laminate, indicating ply volume fractions and magnitudes of in-plane stiffness coefficients as functions of the volume fraction c_{45} of the $\pm 45^\circ$ plies. The 0° fibers and the x_1-axis of the laminate are parallel to the X_3 or z-axis of the cylinder.

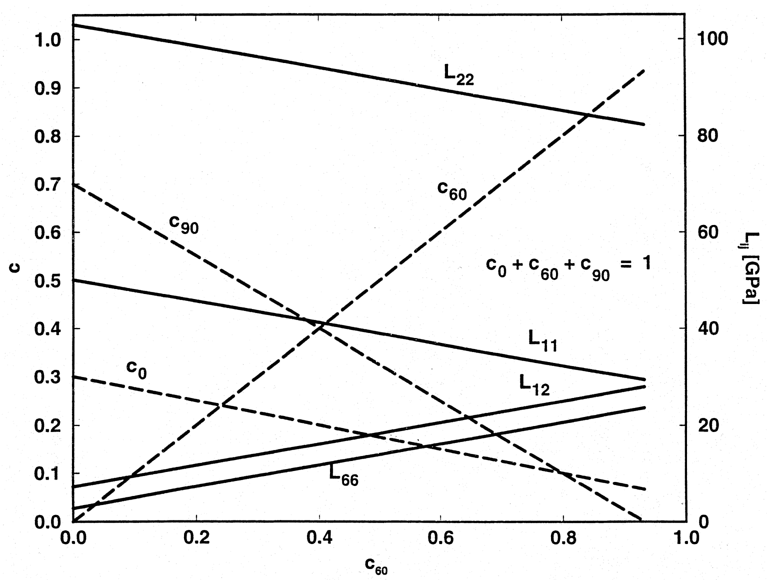

Fig. 3. Design diagram for a $(0_{c_0}/60_{c_{60}}/90_{c_{90}})$, AS4/3501-6 laminate, indicating ply volume fractions and magnitudes of in-plane stiffness coefficients as functions of the volume fraction c_{60} of the $\pm 60^\circ$ plies. The 0° fibers and the x_1-axis of the laminate are parallel to the X_3 or z-axis of the cylinder.

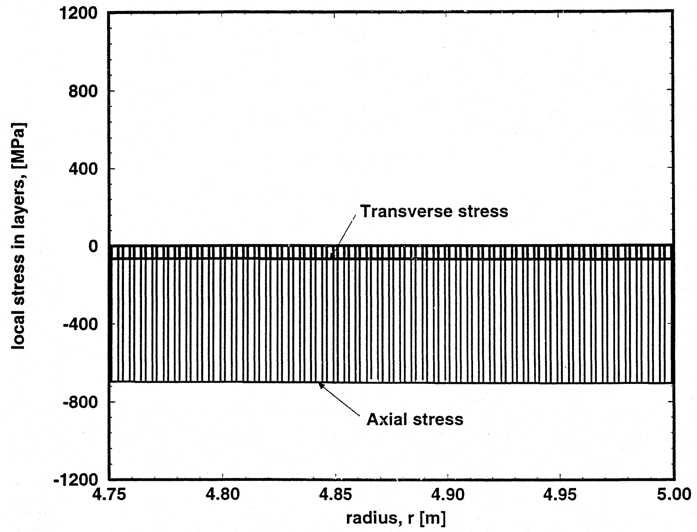

Fig. 4. Axial and transverse stresses in the plies of a 100 layer $(0/\pm 60/90_2)_s$, AS4/3501-6 composite cylinder with closed ends, in the local $x_\alpha x_\beta$-coordinates of each ply. External pressure $p_b = 25$ MPa. External diameter 10 m, wall thickness 0.25 m.

7. Applications

The local fields caused in the layers by the external pressure $p_b = 25$ MPa, acting alone on a closed-end cylinder, were evaluated for a 100 layer $(0/\pm 60/90_2)_s$ laminate made of the AS4/3501-6 composite systems. This layup corresponds to the choice of $c_{60} = 0.4$ in Fig. 3. The cylinder dimensions were selected such that the axial normal stresses in the fiber direction in each layer was equal to about 700 MPa at 25 MPa external pressure, or at the depth of 2500 m. Figure 4 shows the ply stresses in the local coordinates of each ply. As expected, both the axial and transverse local normal stresses are nearly uniform through the wall thickness. Figures 5 and 6 show the same ply stresses replotted in the global $r\theta z$ coordinates of the cylinder (Fig. 1). Due to the dissimilar ply orientation, these stresses show considerable variation from ply to ply.

Another result of interest is the distribution of ply stresses caused by a uniform change in temperature of the structure. The cylinder dimensions, laminate layup and material system are the same as those in Figs 3–5. For the $\Delta T = 1°$C, the largest stress is the hoop stress $\sigma_{\theta\theta} = 0.62$ MPa in the 90° plies (Fig. 7) with the fibers oriented in the θ-direction. The normal stresses in the z-direction of the cylinder axis were one order of magnitude smaller. This indicates that the thermal stresses encountered in normal operations are likely to be small. However, more significant thermal stresses would be caused if the entire cylinder was cooled uniformly from a curing temperature of 120–175°C. This can be the case in manufacture of relatively small test specimens.

Finally, the stress distributions due to uniform eigenstrains in layers are also obtained. The purpose here is to examine the self-stress caused by a uniform eigenstrain in any particular layer and also its influence on other layers. This is better demonstrated by considering the same cylinder described earlier in this section but with only ten layers of $(0/\pm 60/90_2)_s$ layup and equal thickness.

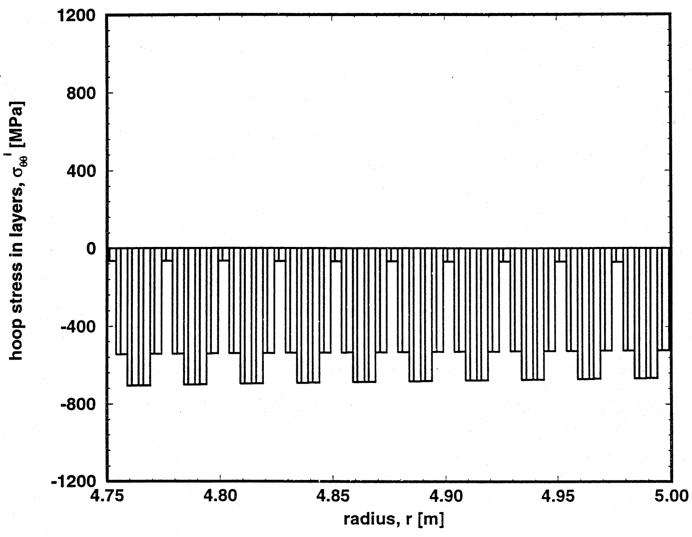

Fig. 5. The $\sigma_{\theta\theta}$ hoop stresses in the plies of a 100 layer $(0/\pm 60/90_2)_s$, AS4/3501-6 composite cylinder with closed ends, in the global coordinates of Fig. 1. External pressure $p_b = 25$ MPa. External diameter 10 m, wall thickness 0.25 m.

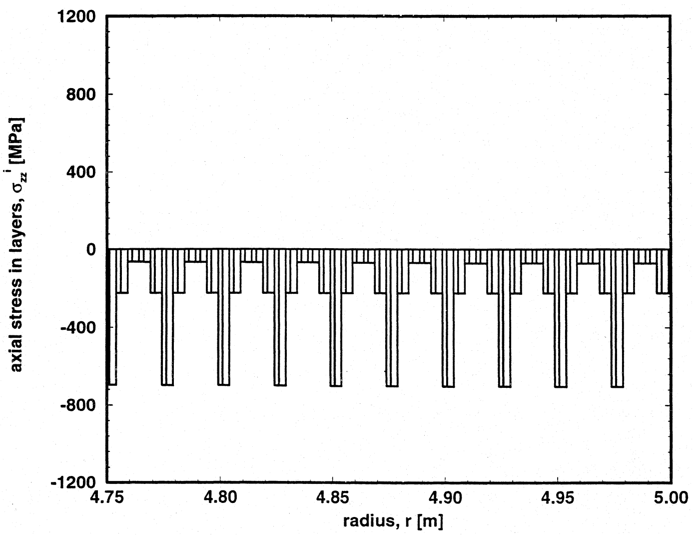

Fig. 6. The σ_{zz} axial stresses in the plies of a 100 layer $(0/\pm 60/90_2)_s$, AS4/3501-6 composite cylinder with closed ends, in the global coordinates of Fig. 1. External pressure $p_b = 25$ MPa. External diameter 10 m, wall thickness 0.25 m.

An eigenstrain component $\mu^j_{\theta\theta} = 1\times 10^{-6}$ or $\mu^j_{zz} = 1\times 10^{-6}$ is applied in one layer at a time and the stresses in layers are evaluated each time from eqns (29), (32) and (61).

Figures 8–10 show the direct effect on hoop stresses in plies by hoop eigenstrain component $\mu_{\theta\theta}$ in the 0 (layer 1), 60 (layer 2) and 90 (layer 4) degree layers. In all the cases, the self-stress is compressive while the residual stresses on other layers are tensile and of comparatively lesser

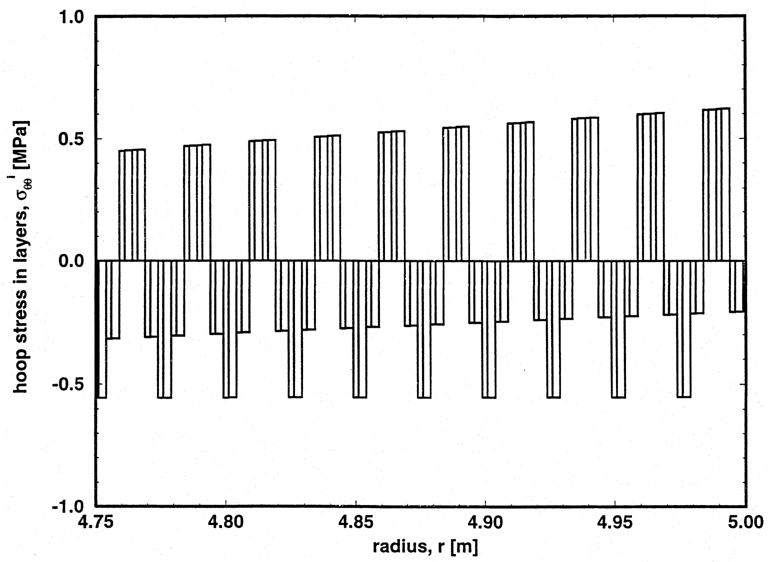

Fig. 7. The $\sigma_{\theta\theta}$ hoop stresses in the plies of a 100 layer $(0/\pm 60/90_2)_s$, AS4/3501-6 composite cylinder with closed ends, in the global coordinates of Fig. 1. Uniform change in temperature $\Delta T = 1°C$. Zero external pressure. External diameter 10 m, wall thickness 0.25 m.

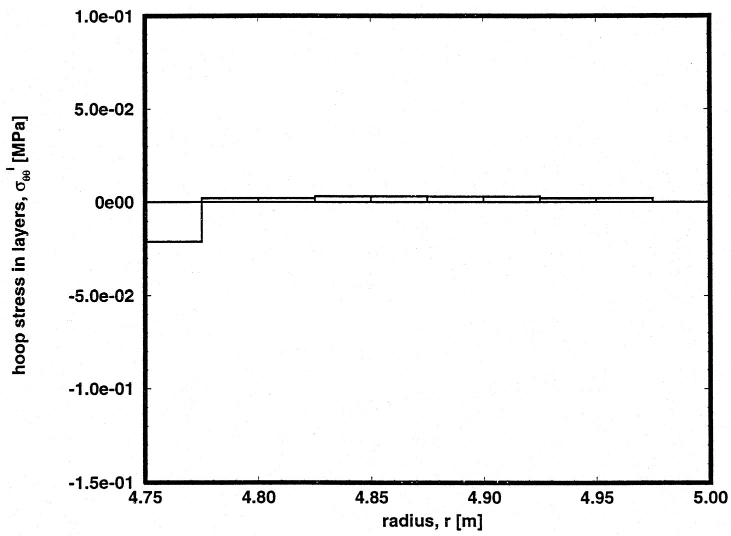

Fig. 8. The $\sigma_{\theta\theta}$ hoop stresses in the plies of a 10 layer $(0/\pm 60/90_2)_s$, AS4/3501-6 composite cylinder with closed ends, in the global coordinates of Fig. 1. Uniform eigenstrain $\mu_{\theta\theta}^{(1)} = 1 \times 10^{-6}$, in 0° layer (layer 1). Zero external pressure. External diameter 10 m, wall thickness 0.25 m.

magnitude than the self-stress. The magnitude of the compressive self stress is higher in 90° layer compared to 60° layer, which in turn, is higher than that in the 0° layer because the hoop stiffness

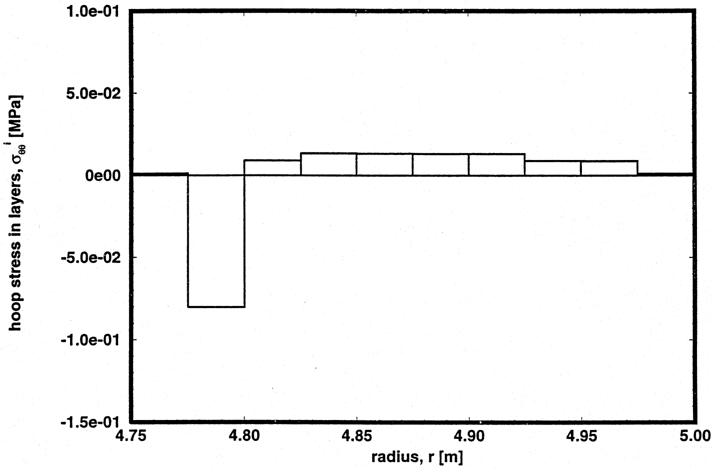

Fig. 9. The $\sigma_{\theta\theta}$ hoop stresses in the plies of a 10 layer $(0/\pm 60/90_2)_s$, AS4/3501-6 composite cylinder with closed ends, in the global coordinates of Fig. 1. Uniform eigenstrain $\mu_{\theta\theta}^{(2)} = 1\times 10^{-6}$, in 60° layer (layer 2). Zero external pressure. External diameter 10 m, wall thickness 0.25 m.

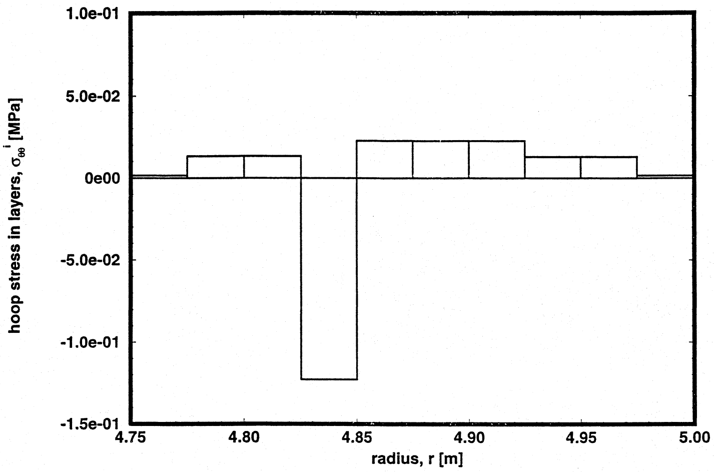

Fig. 10. The $\sigma_{\theta\theta}$ hoop stresses in the plies of a 10 layer $(0/\pm 60/90_2)_s$, AS4/3501-6 composite cylinder with closed ends, in the global coordinates of Fig. 1. Uniform eigenstrain $\mu_{\theta\theta}^{(4)} = 1\times 10^{-6}$, in 90° layer (layer 4). Zero external pressure. External diameter 10 m, wall thickness 0.25 m.

in these layers decreases in that order. The cross effect of hoop eigenstrain on axial stresses in layers is negligible.

The axial residual stress distributions due to axial eigenstrains in the 0, 60 and 90° layers are shown in Figs 11–13. Again, in all the cases, the self stresses are compressive and the residual stresses are tensile. Appreciable tensile residual stress are caused only in the stiffer 0° layers. The cross effects due to axial eigenstrain were also found to be negligible.

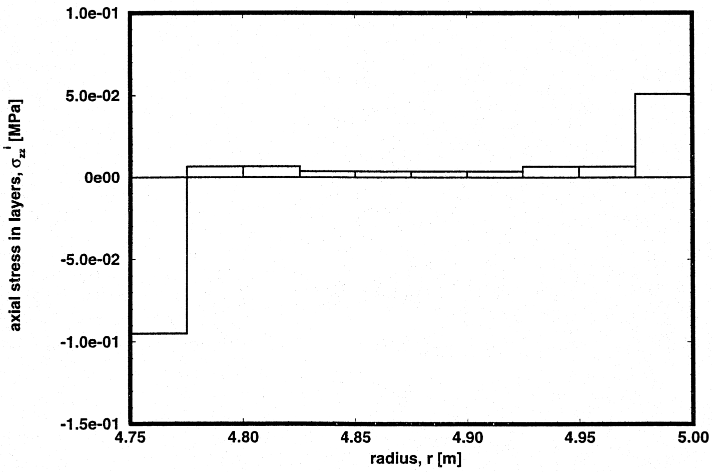

Fig. 11. The σ_{zz} axial stresses in the plies of a 10 layer $(0/\pm 60/90_2)_s$, AS4/3501-6 composite cylinder with closed ends, in the global coordinates of Fig. 1. Uniform eigenstrain $\mu_{zz}^{(1)} = 1\times10^{-6}$, in 0° layer (layer 1). Zero external pressure. External diameter 10 m, wall thickness 0.25 m.

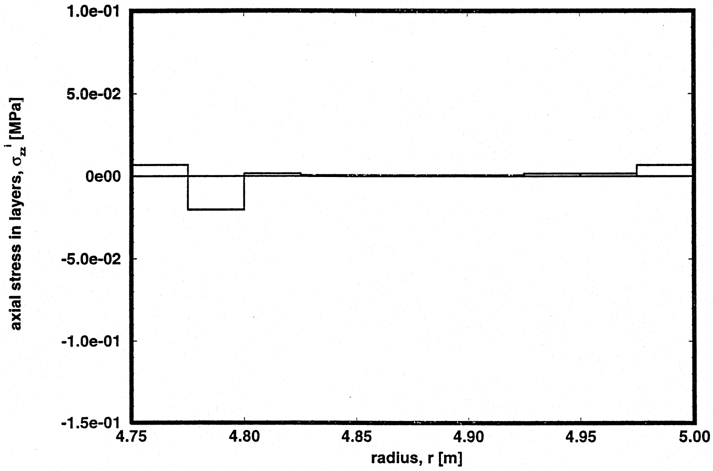

Fig. 12. The σ_{zz} axial stresses in the plies of a 10 layer $(0/\pm 60/90_2)_s$, AS4/3501-6 composite cylinder with closed ends, in the global coordinates of Fig. 1. Uniform eigenstrain $\mu_{zz}^{(2)} = 1\times10^{-6}$, in 60° layer (layer 2). Zero external pressure. External diameter 10 m, wall thickness 0.25 m.

8. Closure

The results derived here provide, in part, a theoretical foundation for the fabrication process analysis of the cylindrical laminate that is presented in the sequel. Also, they show a simple procedure for selection of a laminate layup that distributes equally among the plies the stresses caused by the hydrostatic pressure. Use of other layups is of course possible, but leads to inefficient use of the composite material.

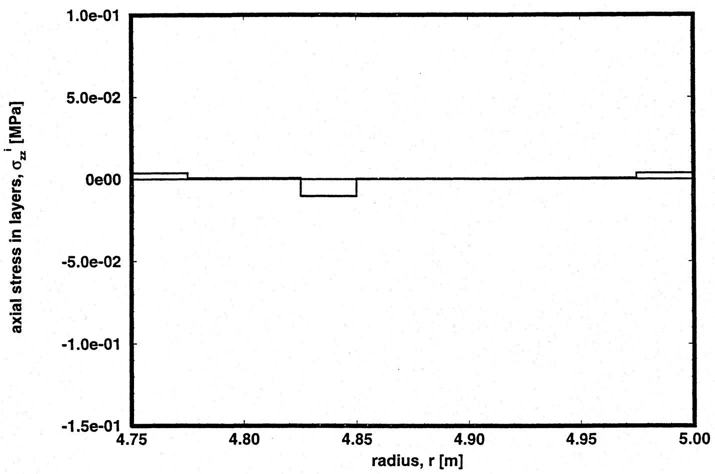

Fig. 13. The σ_{zz} axial stresses in the plies of a 10 layer $(0/\pm 60/90_2)_s$, AS4/3501-6 composite cylinder with closed ends, in the global coordinates of Fig. 1. Uniform eigenstrain $\mu_{zz}^{(4)} = 1\times 10^{-6}$, in 90° layer (layer 4). Zero external pressure. External diameter 10 m, wall thickness 0.25 m.

Moreover, the stresses generated by a uniform change in temperature of the laminate are shown to be small at ordinary operating conditions. However, they can become significant under the large changes applied during cooling from the curing temperature of 120–175°C. Of course, such heating/cooling cycles can be applied only to relatively small fiber-wound cylindrical test specimens, whereas large structures produced by fiber placement techniques may see only local temperature changes causing much less significant residual thermal stresses; this is discussed in Part II. Finally, the effect of uniform layer eigenstrain components on the residual stresses is examined in a 10-ply cylinder. The direct effect of both the hoop and axial components on the corresponding stress components is found to be the most significant. However, equilibrium of axial tractions causes appreciable axial normal stresses in the stiff 0° plies. Cross-effects are not significant.

Acknowledgements

This work was supported by the Ship Structures and Systems S&T Division of the Office of Naval Research; Dr Yapa D. S. Rajapakse served as program monitor.

Appendix

The coefficient matrices $\boldsymbol{k}^j$, $\boldsymbol{q}^j$, $\boldsymbol{s}^j$ and $\boldsymbol{w}^j$ appearing in eqns (28) and (29) are listed here. We start with definitions of various constants that simplify the expressions

$$D_1^j = L_{r\theta}^j + k_j L_{rr}^j \quad D_2^j = L_{r\theta}^j - k_j L_{rr}^j \quad D_3^j = L_{rz}^j - (L_{rr}^j + L_{r\theta}^j)\mathscr{C}^j$$

$$E_1^j = L_{\theta\theta}^j + k_j L_{r\theta}^j \quad E_2^j = L_{\theta\theta}^j - k_j L_{r\theta}^j \quad E_3^j = L_{\theta z}^j - (L_{r\theta}^j + L_{\theta\theta}^j)\mathscr{C}^j$$

$$F_1^j = L_{\theta z}^j + k_j L_{rz}^j \quad F_2^j = L_{\theta z}^j - k_j L_{rz}^j \quad F_3^j = L_{zz}^j - (L_{rz}^j + L_{\theta z}^j)\mathscr{C}^j \tag{77}$$

where the coefficients of $\boldsymbol{L}^j$ are defined in (4)–(7), $\mathscr{C}^j$ is given in (13) and as in (11), $k_j^2 = L_{\theta\theta}^j / L_{rr}^j$.

Evaluation of layer stress averages in (26) involves the integrals

$$I_1^j = \frac{1}{b_j - a_j} \int_{a_j}^{b_j} \xi_j^{k_j - 1} \, \mathrm{d}r_j = \frac{1 - c_j^{k_j}}{k_j(1 - c_j)} \tag{78}$$

$$I_2^j = \frac{1}{b_j - a_j} \int_{a_j}^{b_j} \xi_j^{-k_j - 1} \, \mathrm{d}r_j = \frac{c_j^{-k_j} - 1}{k_j(1 - c_j)} \tag{79}$$

$$I_3^j = \frac{1}{b_j - a_j} \int_{a_j}^{b_j} \xi_j^{-2} \, \mathrm{d}r_j = \frac{1}{c_j} \tag{80}$$

$$I_4^j = \frac{1}{b_j - a_j} \int_{a_j}^{b_j} \log(\xi_j b_j) \, \mathrm{d}r_j = \frac{1}{(1 - c_j)} [(\log b_j - 1) - c_j(\log a_j - 1)] \tag{81}$$

$$J_1^j = \frac{1}{V_j} \int_{V_j} \xi_j^{k_j - 1} \, \mathrm{d}V_j = 2 \frac{1 - c_j^{k_j + 1}}{(1 + k_j)(1 - c_j^2)} \tag{82}$$

$$J_2^j = \frac{1}{V_j} \int_{V_j} \xi_j^{-k_j - 1} \, \mathrm{d}V_j = 2 \frac{1 - c_j^{-k_j + 1}}{(1 - k_j)(1 - c_j^2)} \tag{83}$$

$$J_3^j = \frac{1}{V_j} \int_{V_j} \xi_j^{-2} \, \mathrm{d}V_j = -2 \frac{\log c_j}{(1 - c_j^2)} \tag{84}$$

$$J_4^j = \frac{1}{V_j} \int_{V_j} \log(\xi_j b_j) \, \mathrm{d}V_j = \frac{1}{2(1 - c_j^2)} [(2 \log b_j - 1) - c_j^2 (2 \log a_j - 1)] \tag{85}$$

Next, we recall the constants $\mathscr{U}^j$, $\mathscr{B}^j$, $\mathscr{C}^j$, $\mathscr{E}^j$ and $\mathscr{F}^j$ defined with (13) and (14), and denote

$$\mathscr{U}_1^j = \mathscr{U}^j (c_j^{k_j + 1} - 1) \qquad \mathscr{U}_2^j = \mathscr{U}^j (c_j^{2k_j} - c_j^{k_j + 1})$$

$$\mathscr{B}_1^j = \mathscr{B}^j (c_j^{k_j + 1} - 1) \qquad \mathscr{B}_2^j = \mathscr{B}^j (c_j^{2k_j} - c_j^{k_j + 1})$$

$$\mathscr{C}_1^j = \mathscr{C}^j (c_j^{k_j + 1} - 1) \qquad \mathscr{C}_2^j = \mathscr{C}^j (c_j^{2k_j} - c_j^{k_j + 1})$$

$$\mathscr{E}_1^j = \frac{\mathscr{E}^j}{2} [c_j^2 (2 \log a_j - 1) - (2 \log b_j - 1)]$$

$$\mathscr{E}_2^j = \frac{\mathscr{E}^j}{2} [(2 \log b_j - 1) - (2 \log a_j - 1)]$$

$$\mathscr{F}_1^j = \frac{\mathscr{F}^j}{2} [c_j^2 (2 \log a_j - 1) - (2 \log b_j - 1)]$$

$$\mathscr{F}^j_2 = \frac{\mathscr{F}^j}{2}[(2\log b_j - 1) - (2\log a_j - 1)]$$

$$d_j = \frac{1}{(1 - c_j^{2k_j})} \tag{86}$$

This leads us to write the coefficients of $\boldsymbol{k}^j$ in the following form. For $k_j \neq 1$

$$\begin{aligned}
k^j_{11} &= (D^j_1 c_j^{2k_j} - D^j_2)d_j \qquad k^j_{12} = (D^j_2 - D^j_1)c_j^{k_j} d_j \\
k^j_{13} &= a_j[(\mathscr{C}^j_1 D^j_1 c_1^{k_j - 1} + \mathscr{C}^j_2 D^j_2 c_j^{-k_j - 1})d_j - D^j_3] \\
k^j_{21} &= k^j_{12} \qquad k^2_{22} = (D^j_1 - D^j_2 c_j^{2k_j})d_j \\
k_{23} &= -b_j[(\mathscr{C}^j_1 D^j_1 + \mathscr{C}^j_2 D^j_2)d_j - D^j_3] \\
k_{31} &= \frac{1}{a_j}(F^j_2 J^j_2 - F^j_1 J^j_1)c_j^{k_j + 1} V_j d_j \\
k_{32} &= \frac{1}{b_j}(F^j_1 J^j_1 - F^j_2 J^j_2 c_j^{2k_j}) V_j d_j \\
k_{33} &= -[(\mathscr{C}^j_1 F^j_1 J^j_1 + \mathscr{C}^j_2 F^j_2 J^j_2)d_j - F^j_3] V_j
\end{aligned} \tag{87}$$

and for $k_j = 1$,

$$\begin{aligned}
k^j_{11} &= (D^j_1 c_j^2 - D^j_2)d_j \qquad k^j_{12} = (D^j_2 - D^j_1)c_j d_j \\
k^j_{13} &= a_j[(\mathscr{F}^j_1 D^j_1 + \mathscr{F}^j_2 D^j_2)d_j - \Phi^j_1 \log a_j - \Phi^j_2] \\
k^j_{21} &= k^j_{12} \qquad k^j_{22} = (D^j_1 - D^j_2 c_j^2)d_j \\
k_{23} &= -b_j[(\mathscr{F}^j_i D^j_1 + \mathscr{F}^j_2 D^j_2 c_j^2)d_j - \Phi^j_1 \log b_j - \Phi^j_2] \\
k_{31} &= \frac{1}{a_j}(F^j_2 J^j_3 - F^j_1)c_j^2 V_j d_j \\
k_{32} &= \frac{1}{b_j}(F^j_1 - F^j_2 J^j_3 c_j^2) V_j d_j \\
k_{33} &= [-(\mathscr{F}^j_1 F^j_1 + \mathscr{F}^j_2 F^j_2 J^j_3 c_j^2)d_j + \Phi^j_4 J^j_4 + \Phi^j_5] V_j
\end{aligned} \tag{88}$$

The coefficients of $\boldsymbol{q}^j$ are written for $k_j \neq 1$ as

$$\begin{aligned}
q^j_{11} &= -a_j[(\mathscr{U}^j_1 D^j_1 c_j^{k_j - 1} + \mathscr{U}^j_2 D^j_2 c_j^{-k_j - 1})d_j + \Psi_j] \\
q^j_{12} &= -a_j[(\mathscr{B}^j_1 D^j_1 c_j^{k_j - 1} + \mathscr{B}_2 D^j_2 c_j^{-k_j - 1})d_j - \Psi_j] \qquad q^j_{13} = -k^j_{13} \\
q^j_{21} &= b_j[(\mathscr{U}^j_1 D^j_1 + \mathscr{U}^j_2 D^j_2)d_j + \Psi_j] \\
q^j_{22} &= b_j[(\mathscr{B}^j_1 D^j_1 + \mathscr{B}^j_2 D^j_2)d_j - \Psi_j] \qquad q^j_{23} = -k^j_{23}
\end{aligned}$$

$$q^j_{31} = [(\mathscr{U}^j_1 F^j_1 J^j_1 + \mathscr{U}^j_2 F^j_2 J^j_2) d_j - \mathscr{D}_j] V_j$$

$$q^j_{32} = [(\mathscr{B}^j_1 F^j_1 J^j_1 + \mathscr{B}^j_2 F^j_2 J^j_2) d_j + \mathscr{D}_j] V_j \qquad q^j_{33} = -k^j_{33} \tag{89}$$

and for $k_j = 1$, the coefficients become

$$q^j_{11} = -a_j[(\mathscr{E}^j_1 D^j_1 + \mathscr{E}^j_2 D^j_2) d_j + \Psi^j_1 \log a_j + \Psi^j_2]$$

$$q^j_{12} = a_j[(\mathscr{E}^j_1 D^j_1 + \mathscr{E}_2 D^j_2) d_j + \Psi^j_1 \log a_j - \Psi^j_3] \qquad q^j_{13} = -k^j_{13}$$

$$q^j_{21} = b_j[(\mathscr{E}^j_1 D^j_1 + \mathscr{E}^j_2 D^j_2 c_j^2) d_j + \Psi^j_1 \log b_j + \Psi^j_2]$$

$$q^j_{22} = -b_j[(\mathscr{E}^j_1 D^j_1 + \mathscr{E}^j_2 D^j_2 c_j^2) d_j + \Psi^j_1 \log b_j - \Psi^j_3] \qquad q^j_{23} = -k^j_{23}$$

$$q^j_{31} = [(\mathscr{E}^j_1 F^j_1 + \mathscr{E}^j_2 F^j_2 J^j_3 c_j^2) d_j + \Psi^j_4 J^j_4 + \Psi^j_5] V_j$$

$$q^j_{32} = [-(\mathscr{E}^j_1 F^j_1 + \mathscr{E}^j_2 F^j_2 J^j_3 c_j^2) d_j - \Psi^j_4 J^j_4 + \Psi^j_6] V_j \qquad q^j_{33} = -k^j_{33} \tag{90}$$

Finally, the coefficients of $\boldsymbol{s}^j$ and $\boldsymbol{w}^j$ are also evaluated for both cases of k_j. Thus for $k_j \neq 1$

$$s^j_{11} = \frac{d_j}{a_j} c_j^{k_j+1} [D^j_2 I^j_2 - D^j_1 I^j_1]$$

$$s^j_{12} = \frac{d_j}{b_j} [D^j_1 I^j_1 - c_j^{2k_j} D^j_2 I^j_2]$$

$$s^j_{13} = -d_j[\mathscr{C}^j_1 D^j_1 I^j_1 + \mathscr{C}^j_2 D^j_2 I^j_2] + D^j_3$$

$$s^j_{21} = \frac{d_j}{a_j} c_j^{k_j+1} [E^j_2 I^j_2 - E^j_1 I^j_1]$$

$$s^j_{22} = \frac{d_j}{b_j} [E^j_1 I^j_1 - c_j^{2k_j} E^j_2 I^j_2]$$

$$s^j_{23} = -d_j[\mathscr{C}^j_1 E^j_1 I^j_1 + \mathscr{C}^j_2 E^j_2 I^j_2] + E^j_3$$

$$s^j_{31} = \frac{k^j_{31}}{V_j} \quad s^j_{32} = \frac{k^j_{32}}{V_j} \quad s^j_{33} = \frac{k^j_{33}}{V_j} \tag{91}$$

$$w^j_{11} = (\mathscr{U}^j_1 D^j_1 I^j_1 + \mathscr{U}^j_2 D^j_2 I^j_2) d_j + \Psi_j$$

$$w^j_{12} = (\mathscr{B}^j_1 D^j_1 I^j_1 + \mathscr{B}^j_2 D^j_2 I^j_2) d_j - \Psi_j \qquad w_{13} = -s_{13}$$

$$w^j_{21} = (\mathscr{U}^j_1 E^j_1 I^j_1 + \mathscr{U}^j_2 E^j_2 I^j_2) d_j + \Psi_j$$

$$w^j_{22} = (\mathscr{B}^j_1 E^j_1 I^j_1 + \mathscr{B}^j_2 E^j_2 I^j_2) d_j - \Psi_j \qquad w^j_{23} = -s_{23}$$

$$w^j_{31} = \frac{q^j_{31}}{V_j} \qquad w^j_{32} = \frac{q^j_{32}}{V_j} \qquad w^j_{33} = \frac{q^j_{33}}{V_j} \tag{92}$$

and for $k_j = 1$

$$
\begin{aligned}
s^j_{11} &= \frac{d_j}{a_j} c_j^2 [D^j_2 I^j_3 - D^j_1] \\
s^j_{12} &= \frac{d_j}{b_j} [D^j_1 - c_j^2 D^j_2 I^j_3] \\
s^j_{13} &= -d_j [\mathscr{F}^j_1 D^j_1 + \mathscr{F}^j_2 D^j_2 I^j_3 c_j^2] + \Phi^j_1 I^j_4 + \Phi^j_2 \\
s^j_{21} &= -\frac{d_j}{a_j} c_j^2 [D^j_1 + D^j_2 I^j_3] \\
s^j_{22} &= \frac{d_j}{b_j} [D^j_1 + c_j^2 D^j_2 I^j_3] \\
s^j_{23} &= -d_j [\mathscr{F}^j_1 D^j_1 - \mathscr{F}^j_2 D^j_2 I^j_3 c_j^2] + \Phi^j_1 I^j_4 + \Phi^j_3 \\
s^j_{31} &= \frac{k^j_{31}}{V_j} \qquad s^j_{32} = \frac{k^j_{32}}{V_j} \qquad s^j_{33} = \frac{k^j_{33}}{V_j}
\end{aligned}
\tag{93}
$$

$$
\begin{aligned}
w^j_{11} &= (\mathscr{E}^j_1 D^j_1 + \mathscr{E}^j_2 D^j_2 I^j_3 c_j^2) d_j + \Psi^j_1 I^j_4 + \Psi^j_2 \\
w^j_{12} &= -(\mathscr{E}^j_1 D^j_1 + \mathscr{E}_2 D^j_2 I^j_3 c_j^2) d_j - \Psi^j_1 I^j_4 + \Psi^j_3 \qquad w_{13} = -s_{13} \\
w^j_{21} &= (\mathscr{E}^j_1 D^j_1 - \mathscr{E}^j_2 D^j_2 I^j_3 c_j^2) d_j + \Psi^j_1 I^j_4 + \Psi^j_3 \\
w^j_{22} &= -(\mathscr{E}^j_1 D^j_1 - \mathscr{E}^j_2 D^j_2 I^j_3 c_j^2) d_j - \Psi^j_1 I^j_4 + \Psi^j_2 \qquad w^j_{23} = -s_{23} \\
w^j_{31} &= \frac{q^j_{31}}{V_j} \qquad w^j_{32} = \frac{q^j_{32}}{V_j} \qquad w^j_{33} = \frac{q^j_{33}}{V_j}
\end{aligned}
\tag{94}
$$

References

Christensen, R.M., 1979. Mechanics of Composite Materials. John Wiley, New York.

Daniel, I.M., Ishai, O., 1994. Engineering Mechanics of Composite Materials. Oxford University Press, New York.

Dvorak, G.J., 1992. Transformation field analysis of inelastic composite materials. Proc. R. Soc. Lond. A437, 311–327.

Dvorak, G.J., Benveniste, Y., 1992. On transformation strains and uniform fields in multiphase elastic media. Proc. R. Soc. Lond. A437, 291–310.

Dvorak, G.J., Prochazka, P., 1996. Thick-walled composite cylinders with optimal fiber prestress. Composites Part B 27B, 643–649.

Kardomateas, G.A., 1997. Koiter-based solution for the initial post-buckling behavior of moderately thick orthotropic and shear deformable cylindrical shells under external pressure. J. App. Mech. 64, 885–896.

Kardomateas, G.A., Philobox, M.S., 1995. Buckling of thick orthotropic cylindrical shells under combined external pressure and axial compression. AIAA J. 33, 1946–1953.

Luo, J., Sun, C. T., 1991. Global-local methods for thermoelastic analysis of thick fiber-wound cylinders. J. Composite Materials 25, 453–468.

Srinivas, M.V., Dvorak, G.J., Prochazka, P., 1999. Design and fabrication of submerged cylindrical laminates—II. Effect of fiber pre-stress. Int. J. Solids Structures 36, 3945–3976.

Sun, C.T., Li, S. 1988. Three-dimensional effective elastic constants for thick laminates. J. Composite Materials 22, 629–639.